Abstract Volume
6th Swiss Geoscience Meeting

Lugano, 21st – 23rd November 2008

Apply! Geosciences
6th Swiss Geoscience Meeting 2008 - Lugano

sc | nat

Geosciences
Platform of the Swiss Academy of Sciences

SUPSI
University of Applied Sciences
of Southern Switzerland
Institute of Earth Sciences

4. Meteorology and Climatology (open session)

Rolf Philipona, Markus Furger

Swiss Meteorological Society

4.1 Barthazy E.: Electron microscopy of aerosols

4.2 Füllemann C., Begert M., Brönnimann S., Croci-Maspoli M.: Digitization and homogenization of long-term climate series from surface observation stations in Switzerland - DigiHom

4.3 Hering A., German U., Boscacci M.: Operational nowcasting of thunderstroms in the Alps using TRT during MAP D-PHASE

4.4 Jelex D., Kuc T., Necki J., Rozanski K., Zimnoch M. : Assessing fossil fuel CO_2 fluxes in the urban atmosphere of the city using combined measurements of CO_2, CO and $^{14}CO_2/^{12}CO_2$ mixing ratios

4.5 Morland J., Collaud Coen M., Hocke K., Jeannet P., Mätzler C.: Changes in integrated water vapor above Switzerland over the last 12 years

4.6 Perler D., Geiger A., Leuenberger D., Brockmann E., Kahle H.-G.: Impact of GNSS network design on water vapour tomography

4.7 Philipona R., Behrens K., Ruckstuhl C.: How declining aerosols and rising greenhouse gases forced rapid warming in Europe since the 1980s

4.8 Roesli H.P.: Monitoring weather/climate related and other phenomena by simple RGB compositing of multispectral imagery from Meteosat Second Generation

4.9 Vogt R., Frey C.M., Burri S., Harhash M., Parlow E.: Eddy covariance measurment of CO_2-fluxes in Cairo/Egypt

4.10 Wach P., Zimnoch M., Rozanski K., Kozak K. : Temporal variability of Radon-222 in near-ground atmosphere

4.11 Walker D., Vuilleumier L.: Effect of clouds on erythemal UV radiation

4.1

Electron microscopy of aerosols

Barthazy Eszter

ETH Zürich, Institut für Atmosphäre und Klima, Universitätsstrasse 16, 8092 Zürich
Und
Elektronenmikroskopie Zentrum ETH Zürich, Wolfgang-Pauli-Strasse 16, 8093 Zürich
(eszter.barthazy@emez.ethz.ch)

The CIRRUS-III field experiment took place in November 2006 in Northern Germany. The objective of the campaign was to investigate midlatitude frontal cirrus clouds and the environment in which they form in order to better understand their formation mechanisms. Measurements were made with the enviscope Learjet. Six flights were conducted over the altitude range from 7-12 km, corresponding to the upper troposphere/lower stratosphere. Aerosols were sampled on TEM grids for analysis in a transmission electron microscope.

The aerosol samples were investigated with a Philips transmission electron microscope CM30, working with 300 kV. Results are shown of aerosols sampled in dry air, within clouds and from a flight through stratospheric air. Size distributions were analysed as well as the composition according to different aerosol types. Sulfuric acid aerosols were abundant in in-cloud samples. One sample showed almost exclusively soot particles. Organics and mineral dust aerosols were less frequent. The type of the aerosols were determined using EDX (electron dispersive X-ray spectrometer) by identifying the elemental composition of single aerosols.

4.2

Digitization and homogenization of long-term climate series from surface observation stations in Switzerland – DigiHom

Füllemann Christine*, Begert Michael*, Brönnimann Stefan**, Croci-Maspoli Mischa*

**Swiss Federal Office of Meteorology and Climatology MeteoSwiss, Krähbühlstrasse 58, CH-8044 Zurich (christine.fuellemann@meteoswiss.ch)*
*** Swiss Federal Institute of Technology, Institute for Atmospheric and Climate Science, Universitätstrasse 16, CH-8092 Zurich*

The term DigiHom combines the intentions at MeteoSwiss i) to digitize long-term surface time-series from historical paper data and ii) to homogenize the complete data series with respect to make accurate estimates of the dimension of climate change and the corresponding effects. The goal of DigiHom is to make an important contribution to the national and international climate observation system by means of long-term climate series of Switzerland.
DigiHom has a time-frame from 2008-2011 and is accomplished in close collaboration with ETH Zurich who has profound experience in the digitization process (Brönnimann et al., 2006). The homogenization process will be carried out at MeteoSwiss using a well established homogenization procedure (THOMAS, Tool for Homogenization of monthly data series, cf. Begert et al. 2005).
The surface observation stations processed within DigiHom are the long–term climate series of the newly defined Swiss National Basic Climatological Network (Swiss NBCN). This network defines the most valuable climatological stations in Switzerland and accordingly guarantees a long-term perspective of their operation. The Swiss NBCN consists of 28 climatological stations (different parameters), presented in Begert et al. (2007) and 46 precipitations stations (Begert, 2008) covering respectively all climatological regions of Switzerland (Fig. 1). Representative climatological regions for the different surface observation stations have been calculated using the complete-linkage cluster analysis.
After the successful completion of DigiHom in 2010 the following climatological variables will be available electronically and in high-quality back to the year of their origin (most of them before 1900): temperature (mean, minimum, maximum), precipitation and sunshine duration. Although the coverage of stations at different altitudes is quite good, stations with multivariate time series are mainly located below 1000m asl (see Fig. 2). Higher elevated stations generally offer mean temperature and precipitation series. 6 NBCN stations have all parameters starting before 1901.
In this study the technical background to accomplish DigiHom will be presented and first results of homogenized long-term time-series will be introduced.

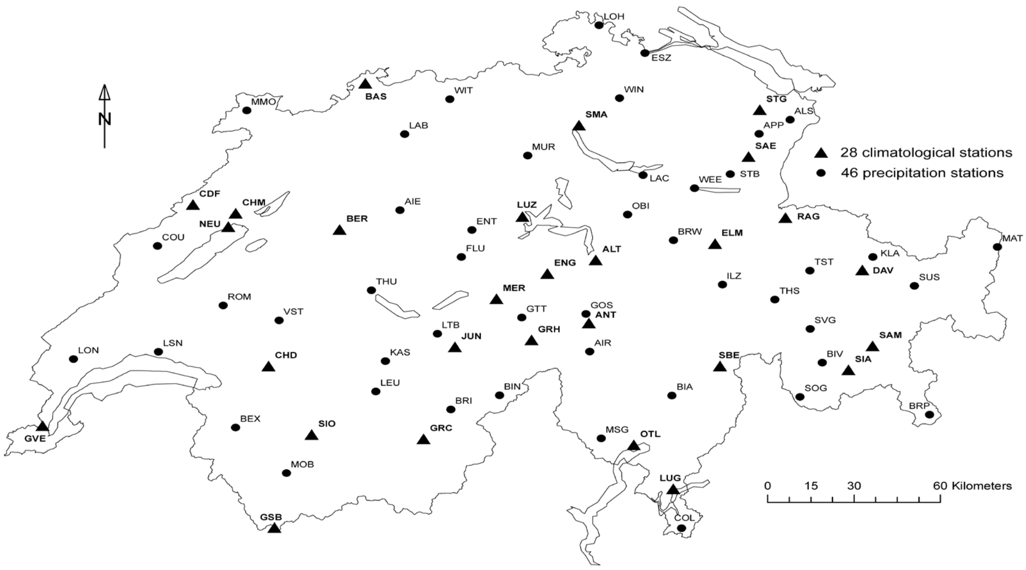

Figure 1. The 74 NBCN surface observation stations in Switzerland separated as 28 climatological stations (different parameters) and 46 precipitation stations.

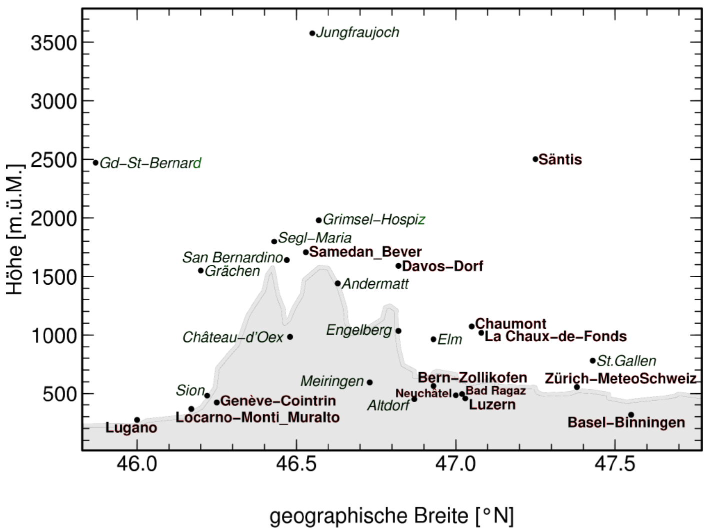

Figure 2. Distribution of the 28 climatological NBCN stations in relation to latitude and altitude.

REFERENCES

Begert M., Schlegel T., Kirchhofer W. 2005: Homogeneous temperature and precipitation series of Switzerland from 1864 to 2000. Int. J. Climatol. 25, 65-80.

Begert, M., Seiz, G., Foppa, N., Schlegel, T., Appenzeller, C., Müller, G. 2007: Die Überführung der klimatologischen Referenzstationen der Schweiz in das Swiss National Climatologial Network (Swiss NBCN), Arbeitsberichte der MeteoSchweiz, 215, 43p.

Begert, M. 2008: Repräsentativität der Stationen im Swiss National Basic Climatological Network. Arbeitsberichte der MeteoSchweiz, 217, 40p.

Brönnimann, S., Annis, J., Dann, W., Ewen, T., Grant, A. N., Griesser, T., Krähenmann, S., Mohr, C., Scherer M., Vogler C. 2006: A guide for digitising manuscript climate data. Climate of the Past, 2, 137-144.

4.3

Operational nowcasting of thunderstorms in the Alps using TRT during MAP D-PHASE

Hering Alessandro, Germann Urs & Boscacci Marco

Swiss Federal Office of Meteorology and Climatology (MeteoSwiss), Via ai Monti 146, CH-6605 Locarno-Monti, (alessandro.hering@meteoswiss.ch)

The MAP Forecast Demonstration Project D-PHASE was an excellent opportunity to demonstrate in real-time the performance of the operational nowcasting system TRT (Thunderstorms Radar Tracking). Since 2003 MeteoSwiss runs this real-time object-oriented nowcasting tool, as a part of its severe thunderstorms nowcasting, warning and information system. TRT is a multiple-radar, multiple-sensor system that uses heuristic and centroid-based methods for the automatic detection, tracking, characterisation and extrapolation of intense convective cells. TRT was used during MAP D-PHASE as one of the operational nowcasting systems in the Alpine area, and was available in real-time on the project visualisation platform.

The current version of TRT fully exploits volumetric reflectivity data of multiple-radar composites to describe the 3D storm structure, and has been expanded to a multiple-sensors system including cloud-to-ground lightning flashes. TRT is tuned to identify individual cells rather than storm systems, hence the evolution of cell-based attributes like e.g. VIL (Vertically Integrated Liquid), 15/45 dBZ echo tops, the altitude of maximum storm reflectivity, and cloud-to-ground lightning flashes is available to the forecasters in real-time.

The latest improvement in TRT is the "cell severity ranking" nowcasting product, developed for MAP D-PHASE and tested in real-time on the visualisation platform during the demonstration period from June to November 2007. The goal of this product is to find and highlight the most dangerous and strongest cells, and to enhance the reliability and timeliness of severe convection warnings. To this purpose thunderstorm cells are classified into four distinct categories based on their severity and represented by a colour coded ellipse. The severity categories are computed integrating the three cell-based attributes VIL, mean of 45 dBZ Echo Top altitude, and maximum cell reflectivity, with a weighting scheme.

The new product includes also a 60 minutes position forecast. The estimated future position of the thunderstorms is computed based on the motion of individual cells, using their weighted displacement velocities. The expected position is shown with a colour coded ellipse and takes into account the spread (standard deviation) of the velocity vectors from the last three 5min time steps. The size of the ellipse is proportional to the uncertainty of the position forecast.

The presentation will focus on the added value of the new cell severity ranking product, which combines together the 3D-radar attributes VIL, 45 dBZ Echo Top, and maximum reflectivity.

4.4

Assessing fossil fuel CO_2 fluxes in the urban atmosphere of the city using combined measurements of CO_2, CO and $^{14}CO_2/^{12}CO_2$ mixing ratios

Jelen Dorota, Kuc Tadeusz, Necki Jaroslaw, Rozanski Kazimierz, Zimnoch Miroslaw

AGH University of Science and Technology, Al. Mickiewicza 30, 30 – 059 Krakow, Poland (djelen@novell.ftj.agh.edu.pl)

Emissions of carbon dioxide related to burning of fossil fuels constitute an important component of the carbon budget, both on global and regional scales. For heavily industrialized and populated areas such as western and central Europe, a large proportion of the total CO_2 flux entering the atmosphere is attributed to this source. Global and regional models of carbon cycle rely mainly on emission statistics to quantify the magnitude and variability of the fossil CO_2 flux into the atmosphere.

Krakow (50°04'N, 19°55'E, 220 m a.s.l.) is a large urban agglomeration located in the southern Poland, with about 1 million inhabitants, rapidly growing car traffic and significant industrial activities. Consumption of coal, gas and oil for communal and transport purposes generates major fluxes of anthropogenic carbon dioxide and carbon monoxide within the region. In addition, due to prevailing westerly air circulation, the Krakow region is under substantial influence of a large coal mining and industrial centre (Upper Silesia) located approximately 60 km west of the city.

The $^{14}CO_2/^{12}CO_2$ ratios measured in Krakow since 1983 testify major changes in economy of the region which have occurred since 1989. The ^{14}C signature of atmospheric CO_2 reflects significant changes in anthropogenic CO_2 fluxes released into the atmosphere both on local and regional scales. The contribution of fossil-fuel derived CO_2 in the total CO_2 load of the lower atmosphere in Krakow decreased from approximately 21 ppm in 1989 to around 10-12 ppm in the last few years. This change is linked with major reduction in coal consumption in Poland, from ca. 160 Mt in 1985 to 84 Mt in 2004.

The measurements of CO concentrations in urban atmosphere can serve as a substitute for costly determinations of $^{14}CO_2/^{12}CO_2$ mixing ratios, provided that the ratio CO/CO_2(fossil) is determined for the given area and its variability is adequately characterized. The average value of CO/CO_2(fossil) ratio derived for the period April 2003 - April 2006 for Krakow region is equal 27.6 ± 4.2 ppb CO per ppm of fossil CO_2. No distinct seasonal changes of this ratio were detected so far. Occasionally, very high (above 70 ppb/ppm) and very low (below 10 ppb/ppm) values of the CO/CO_2(fossil) ratio have been observed. The emission-based CO/CO_2 ratios reported for the period 1998-2005 for major industrial sources in the Krakow region are in the range between 7.3 and 10.8 ppb CO per ppm of fossil CO_2. However, they do not comprise emissions related to car traffic which is an important source of fossil fuel CO_2.

REFERENCES

Kuc, T. Rozanski, K., Zimnoch, M., Necki, J., Chmura, L., Jelen, D. 2007. Two decades of regular observations of $^{14}CO_2$, and $^{13}CO_2$ content in atmospheric carbon dioxide in central Europe: long-term changes of regional anthropogenic fossil CO_2 emissions. Radiocarbon, 49(2), 807-816.

Levin, I., Kromer, B., Schmidt, M. and Sartorius, H. 2003. A novel approach for independent budgeting of fossil fuels CO_2 over Europe by $^{14}CO_2$ observation. Geophys. Lett., 30(23); 2194.

4.5

Changes in integrated water vapor above Switzerland over the last 12 years

Morland June*, Collaud Coen Martine**, Hocke Klemens*, Jeannet Pierre**, Mätzler Christian*

**Institute of Applied Physics, University of Bern, Sidlerstrasse 5, CH-3012 Bern, Switzerland (June.Morland@iap.unibe.ch)*
***MétéoSuisse, Station aérologique, CH-1530 Payerne, Switzerland*

Water vapour is the strongest natural greenhouse gas. Under the assumption of constant relative humidity, the Clausius Clapeyron equation predicts a water vapor increase of 6 % per degree Kelvin increase in atmospheric temperature. Model simulations have shown that the water vapor feedback effect increases the climate sensitivity to rising greenhouse gas concentrations Studies with radiosonde (Ross and Elliott, 2001) and ERA40 (Trenberth et al., 2005) datasets showed large scale trends in Integrated Water Vapour (IWV) of up to +0.04 $mmyr^{-1}$ (+0.13 $\%yr^{-1}$) for the 1975-1995 and 1988-2003 periods, respectively. However, no significant trends were detected over Europe . On the other hand, a study of IWV from 33 ground-based GPS receivers in Sweden and Finland indicated trends of between -0.05 and +0.1 $mmyr^{-1}$ (-0.14 and +0.75 %) with errors of around 0.04 $mmyr^{-1}$ (Nilsson and Elgered, 2008).

Ground based microwave radiometers offer an independent source of atmospheric information from both radiosonde and analysis data. In the present study, IWV was calculated from the TROWARA (TROpospheric WAter RAdiometer) microwave radiometer in Bern for the period 1996-2007. Standard homogenisation techniques (Vincent, 1998) were used to correct for biases caused by instrument problems in the initial period up to 2002. IWV between 850 and 200 hPa was calculated from ECMWF analysis data for the closest gridpoint to Bern. IWV between 850 and 200 hPa, RS (850-200), as well as between the surface and 200 hPa, RS (s-200), was calculated from the Payerne radiosonde data.

Annual trends were calculated using the Least Squares Analysis (LSA) and monthly trends were calculated using the seasonal Mann Kendall (MK) technique following the methods described in Collaud Coen et al, 2007. In the following discussion, trends are given in mm or $\%yr^{-1}$ and the standard error is given afterwards in square brackets. Figure 1 shows the annual trends for all data, midnight and midday datasets calculated using LSA. The TROWARA midday trends are larger than all day or midnight trends, whilst RS and ECMWF data show higher midnight trends. The fact that RS and ECMWF agree more closely than RS and TROWARA is not surprising given the fact that the Payerne radiosonde is assimilated in the ECMWF analysis.

The RS (s-200) midnight trend of +0.087 [0.046] $mmyr^{-1}$ or 0.55 [0.29] $\%yr^{-1}$ is significant at the 90 % level. The TROWARA midday trend (+0.098 [0.061] $mmyr^{-1}$ or 0.70 [0.43] $\%yr^{-1}$) and RS (s -200) trend (+0.068 [0.043] $mmyr^{-1}$ or +0.45 [0.29] $\%yr^{-1}$) for all observations are statistically significant at the 89 % level. These findings are within the range of trends reported by Ross and Elliott (2001), Trenberth et al. (2003) and Nilsson and Elgered (2008). Analysis with the MK technique showed a significant positive trend in July of +0.19 [0.14] to +0.34 [0.25] $mmyr^{-1}$ (+1.2 [0.8] to +1.6 [1.1] $\%yr^{-1}$) for all three datasets. In December, ECMWF and TROWARA indicated a significant negative trend of -0.20 [0.14] and -0.36 [0.24] $mmyr^{-1}$ (-3.6 [2.5] and -4.3 [2.9] $\%yr^{-1}$), respectively. This is consistent with the findings of Nilsson and Elgered (2008), who observed the strongest positive IWV trends in summer and frequently observed negative trends in winter.

The three datasets showed consistent positive annual trends from 1996 to 2007. A longer observing period is needed in order to establish significance, whist observations over several decades are required to distinguish anthropogenic influences from decadal oscillations in the climate system.

REFERENCES

Collaud Coen M., Weingartner, E., Nyeki, S., Cozic, J., Henning, S., Verheggen, B., Gehrig, R. & Baltensperger U. 2007:, Long-term trend analysis of aerosol variables at the high-alpine site Jungfraujoch, J. Geophys. Res., 112, D13213, doi:10.1029/2006JD007995.

Nilsson, T. & Elgered G. 2008: Long Term Trends in the Atmospheric Water Vapor Content Estimated from Ground-Based GPS Data, in Measuring and modelling variations in the distribution of atmospheric water vapour using GPS, Tobias Nilsson, PhD Thesis, Chalmers University of Technology, Göteborg, Sweden.

Ross, R. J.& Elliott W. P. 2001: Radiosonde-Based Northern Hemisphere Tropospheric Water Vapor Trends, J. Clim., 14, 1602-1612.

Trenberth, K. E., Fasullo, J. & Smith L. 2005: Trends and variability in column-integrated atmospheric water vapor, Clim. Dynam, 24(7-8),741-758m doi:10.1007/s00382-005-0017-4.

Vincent, L. A. 1998: A Technique for the Identification of Inhomogeneities in Canadian Temperature Series, J. Clim., 11, 1094-1104.

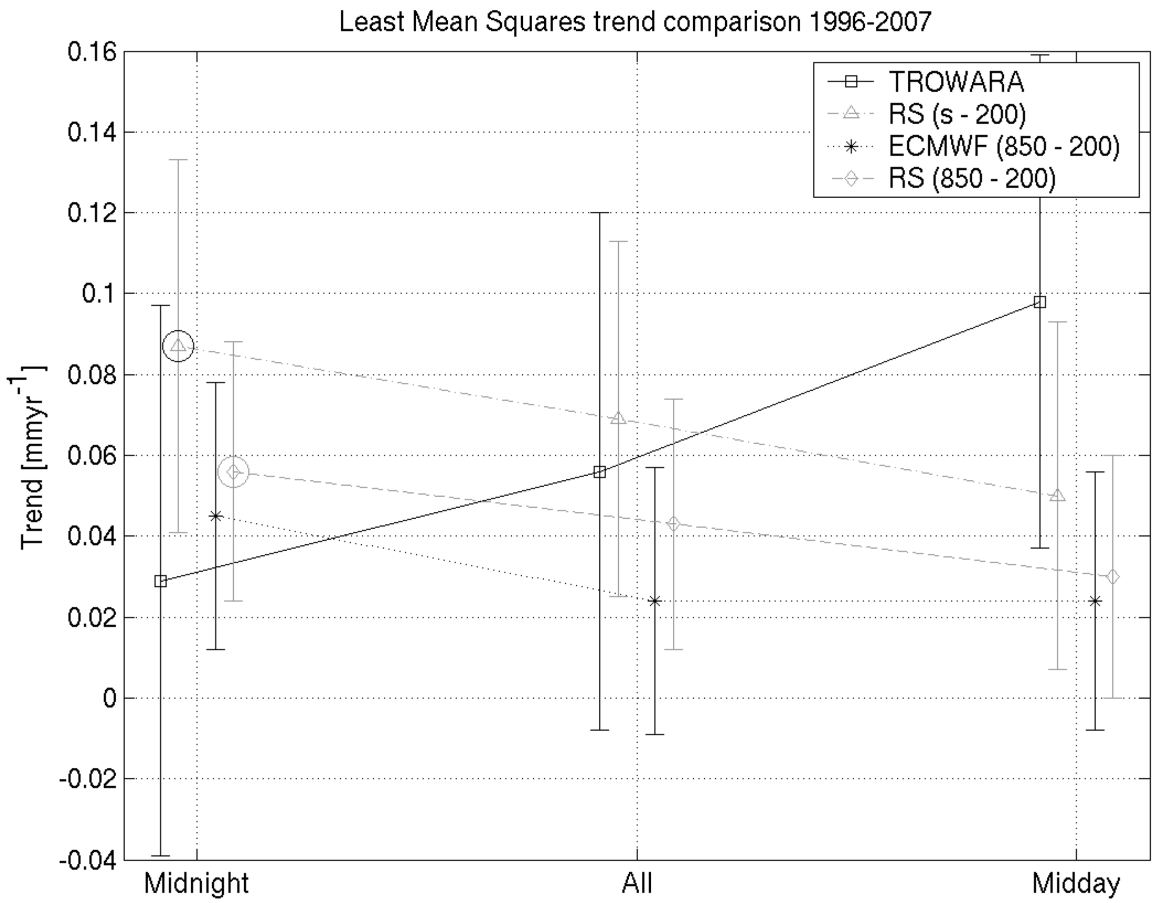

Figure 1. Yearly trends in IWV in mm calculated for the 1996-2007 period. The error bars show the standard error and the large circles indicate that a trend is significant at the 90 % level.

4.6

Impact of GNSS Network Design on Water Vapour Tomography

Perler Donat*, Geiger Alain*, Leuenberger Daniel**, Brockmann Elmar***, Kahle Hans-Gert*

Institute of Geodesy and Photogrammetry, ETH Zurich, Schafmattstrasse 34, CH-8093 Zurich (donat.perler@geod.baug.ethz.ch)
***Federal Office of Meteorology and Climatology MeteoSwiss, Kraehbuehlstrasse 58, CH-8044 Zurich*
****Federal Office of Topography swisstopo, Seftigenstrasse 264, CH-3084 Wabern*

In the last decades, substantial progress is made in Numerical Weather Prediction (NWP). Thanks to the increasing computing power, the model resolution has been continuously ameliorated. In contrast to this, the number of meteorological observations for initialising the models has not evolved to the same extent especially concerning the water vapour measurements over land. The lack of high-resolution water vapour measurements is seen as a major limit for further improvements of the NWPs. With GNSS-tomography, this gap can be filled. GNSS-tomography provides a three dimensional water vapour field with high resolution. Thereby, the setup of the GNSS network is an essential factor for the resolution and for the quality of the provided measurements. Sensitivity analyses are carried out to assess the influence of network configuration and of the visibility of the satellites. Results of network optimisation in view of water vapour tomography will be discussed and presented. The advent and extension of new and existing GNSS, respectively, will allow to simultaneously collect signals from several systems such as GPS, Galileo and GLONASS. The impact of the use of several systems on the result of water vapour tomography is investigated and presented.

4.7

How declining aerosols and rising greenhouse gases forced rapid warming in Europe since the 1980s

Philipona Rolf*, Behrens Klaus**, Ruckstuhl Christian***

* *Federal Office of Meteorology and Climatology MeteoSwiss, Aerological Station, CH-1530 Payerne, Switzerland (rolf.philipona@meteoswiss.ch)*
** *Meteorologisches Observatorium Lindenberg, Deutscher Wetterdienst, D-15848 Lindenberg, Germany*
*** *Institute for Atmospheric and Climate Science, ETH Zürich, CH-8057-Zürich, Switzerland*

Mainland Europe's temperature rise of about 1°C since the 1980s is considerably larger than expected from anthropogenic greenhouse warming. Aerosol optical depth and surface irradiance measurements from radiation sites in Switzerland and Northern Germany, recently showed a 60 % decline of aerosol concentration, which led to a significant increase of solar irradiance under cloud-free skies since the 1980s confirming solar brightening. Here we analyse all shortwave and longwave surface forcings and relate them to humidity- and temperature increases through the radiation- and energy budget over Mainland Europe. Shortwave climate forcings from direct- and indirect- aerosol effects combined are found to be two to three times larger than the longwave forcing from rising anthropogenic greenhouse gases. Almost tree quarters of the energy of these forcings goes into the turbulent fluxes, which increase humidity and hence the longwave forcing by water vapour feedback. However, with respect to the initial anthropogenic forcings the analysis shows that about two thirds of the rapid temperature rise since 1980 is forced by declining aerosols and only one third by rising greenhouse gases. The results explain the recent rapid temperature rise in Europe and demonstrate experimentally how manmade climate forcings increase surface temperature. With aerosol concentrations now reaching low levels in Europe solar brightening likely subsides, and temperature will henceforth mainly increase due to anthropogenic greenhouse warming.

REFERENCES

Ruckstuhl, C., Philipona, R., Behrens, K., Collaud Coen, M., Dürr, B., Heimo, A., Mätzler, C., Nyeki, S., Ohmura, A., Vuilleumier, L., Weller, M., Wehrli, C., and Zelenka, A., 2008: Aerosol and cloud effects on solar brightening and the recent rapid warming, Geophys. Res. Letters, 35, L12708, doi:10.1029/2008GL034228.

4.8

Monitoring weather/climate related and other phenomena by simple RGB compositing of multispectral imagery from Meteosat Second Generation

Roseli HansPeter

via Monte Brè 5, CH-6605 Locarno

Meteosat Second Generation's (MSG) Spinning Enhanced Visible and InfraRed Imager (SEVIRI) provides operationally multispectral imagery at high repetition rate from the geostationary orbit. MSG and SEVIRI have been at their inception in 2002, and still are, a first world-wide in geostationary imaging of the Earth. Since this summer, using the back-up satellite, the northern hemisphere is scanned not only every 15 minutes (full Earth disc by Meteosat-9 at 0° longitude), but also at 5-minute intervals (Meteosat-8 at 9.5° East). The continuous data flow from both satellites allows for excellent monitoring of a wide range of weather/climate related and other phenomena.

Display of individual channels or images of channel differences from a multi-spectral imager falls short of imparting in a concise way to the user the wealth of pertinent information buried in the image data content. Based on experience with AVHRR and MODIS products, the application on SEVIRI image data of the RGB compositing technique offers the possibility of compression of the multi-spectral information content for optimum visualisation, while preserving pattern and texture of cloud, atmosphere and surface features as well as continuity in the time domain. Also, by a careful choice of the inputs to an RGB composite scheme a multitude of phenomena may be captured in one go. Adequately re-projected RGB composites may be used right out to regions on the limb of the SEVIRI coverage. Thus, the RGB compositing technique is an efficient way for a continuous monitoring of phenomena in the atmosphere and on the Earth surface. It preserves the "natural-look-and-feel" of mono-channel imagery many users are used to from earlier satellite generations, in particular when viewing image sequences.

RGB compositing also has its drawbacks. The number of channels invites to a confusing number of possible combinations. There are individual (subtle or more serious) colour perception problems and difficulties in memorising the resulting colour schemes, i.e. in relating colour shades to particular meteorological or non-meteorological features.

For operational applications and for training it is important to reduce the set of RGB schemes to a minimum while maximising the number of identifiable phenomena relevant to the application. At the same time the selected RGB schemes should often cover 24-hours/7-days including twilight conditions with at most small changes in colouring. Most importantly, RGB composting schemes should be based on physical considerations as regards the selection of the channel combinations as well as the attribution of them to the individual colour planes of the RGB display device. This assists in understanding and memorising the image content and its relation to the resulting colour landscape.

A typical RGB example is the 24-hour cloud microphysics RGB. It allows for the identification of fog and low cloud night and day including twilight conditions, while still differentiating among mid/high-level stratiform and convective cloud. In Jython (language used in the display freeware IDV by Unidata) the RGB is coded as follows:

```
# 24-hour cloud microphysics
# units: K
#R:    IR120-IR108     -4K ...   2K
#G:    IR108-IR87       0K ...   6K
#B     IR108          248K ... 303K

def ACMP_RGB(IR87,IR108,IR120):
 R = 255.*max_data(min_data((IR120-IR108+4.)/6.,1.),0.)
 G = 255.*(max_data(min_data((IR108-IR87)/6.,1.),0.)**(1./1.2))
 B = 255.*max_data(min_data((IR108-248.)/55.,1.),0.)
 return combineRGB(R,G,B)
```

RGB composites from SEVIRI data support the identification and monitoring of a multitude of features like:

- solid and liquid water particles (snow – ice crystals – cloud droplets) and of their relative size at, close to, the cloud tops;
- weak-moderate and strong convection;
- air mass type in middle and high troposphere;
- snow and vegetation cover;
- extended flooding;
- dust storms and long-range transport;
- volcanic ash and SO_2 eruption and long-range transport;
- industrial SO_2 release;
- Industrial/wild fire and smoke.

The verbal presentation will show SEVIRI RGB composited images and image sequences covering phenomena from the above list.

4.9

Eddy covariance measurement of CO_2 fluxes in Cairo/Egypt

Vogt Roland, Frey Corinne M., Burri Susanne, Harhash Maha, Parlow Eberhard

Institute of Meteorology, Climatology and Remote Sensing, Basel University
email: Roland.Vogt@unibas.ch

Measurements of CO_2 fluxes in urban areas are still rare, especially when it comes to megacities. As part of a ground truth campaign for a remote sensing project, surface energy balance fluxes were measured at three stations (urban, rural, desert) in and around Cairo, Egypt. At two sites CO_2 fluxes were measured, for details see Frey et al., same conference. In this presentation results from the urban station are reported. It was located at the southern border of the campus of Cairo University in Gizeh (30°01'33.4N, 31°12'27.7E). A 12 m mast was erected on a 20 m high building and attached to a 4.5 m buildup on the flat roof. The flux instrumentation (sonic: Campbell CSAT3, open path gas analyzer: LiCOR LI7500) was mounted on top of the mast. It additionally carried a 4-component net radiometer (Kipp & Zonen CNR1) and a psychrometer. Fluxes were calculated and corrected online, but raw data were also stored for subsequent analysis. The measurement period was from November 10, 2007 to February 26, 2008.
The area north of the station was urban, the area south, south-west was dominated by agricultural use (up to 1 km). To the South-East, there was a sports ground and 400 m to the East the zoo of Cairo was located. The area of the zoo is roughly a 500x1000 m N-S oriented vegetated rectangle. The western bank of the river Nile was 1 km east of the site.
The wind was blowing dominantly from North (60% from N ± 60°, 20% from S ± 40°, from W 16%, from E 4%). Preliminary results show, that on average, the CO_2 flux is upward directed. With winds from South, the magnitude is reduced and can even be downward directed during daytime. Peak values are reached during midday and are in the range of 0.5 to 1.5 mg m^{-2} s^{-1}. Nocturnal values are around 0.2 mg m^{-2} s^{-1}. The weekly traffic intensity can be seen in the CO_2 fluxes. On Fridays there is no distinct diurnal course. Afternoon values are below 0.5 mg m^{-2} s^{-1}. On Saturdays the peaks are slightly reduced with values below 1 mg m^{-2} s^{-1}.

4.10

Temporal variability of Radon-222 in near-ground atmosphere

Wach Paulina*, Zimnoch Miroslaw*, Rozanski Kazimierz*, Kozak Krzysztof**

**AGH University of Science and Technology, Faculty of Physics and Applied Computer Science, al. Mickiewicza 30, 30-059 Krakow, Poland*
***Institute of Nuclear Physics, Laboratory of Radiometric Expertise,*
Radzikowskiego 152, 31-342 Krakow, Poland

Radon-222 is an alpha-emitting radioactive inert gas with the half-life of 3.8 days. It is a product of decay of ^{226}Ra which belongs to ^{238}U-decay series. Uranium-238 and its decay product ^{226}Ra are ubiquitous in the upper Earth's crust and in the soils. Radon-222 which is being released into the pore space of soils, diffuses into the atmosphere where it decays to lead ^{210}Pb through intermediate chain of short-lived radionuclides (^{218}Po-^{214}Pb-^{214}Bi-^{214}Po). The release rate of ^{222}Rn is controlled by source term (^{226}Ra content in the soil and its vertical distribution) and by physical properties of the upper soil layer (mineral structure, porosity, water content).
Concentration of ^{222}Rn has been measured quasi-continuously in Krakow since June 2004 with the aid of radon monitor based on detection of daughter products of this gas. The radon monitor has been calibrated against AlphaGUARD detector. The air intake is located ca. 20 meters above the ground, on the roof of the Faculty building. The radon monitor provides individual readings every 30 minutes, representing average activities of ^{222}Rn over 30-minute sampling intervals. In the same location, quasi-continuous measurements of CO_2 and CH_4 mixing ratios in the local atmosphere are performed.
Rn-222 exhibits substantial seasonal and diurnal fluctuations. The absolute amplitude of the recorded individual ^{222}Rn concentrations reached during the 4-year observation period approximately 40 Bqm^{-3}. The maximum of monthly mean ^{222}Rn concentration occurs usually in October (ca. 10 Bqm^{-3}), while the minimum is recorded in March or April (ca. 2.5 Bqm^{-3}). Daily mean values of ^{222}Rn concentration fluctuate between ca. 1Bqm^{-3} and 18 Bqm^{-3}.
Influence of various factors on the observed variability of ^{222}Rn concentration in the near-ground atmosphere in Krakow on different time scales (diurnal, synoptic, seasonal) was investigated. The following parameters were considered: (I) stability of the lower atmosphere largely controlling diurnal variability, (II) wind speed, (III) temperature, (IV) fluctuations of atmospheric pressure, (V) history of air masses, (VI) fluctuations of water table and water content of the soil column.

4.11
Effect of clouds on erythemal UV radiation

Walker Daniel[*] [**], Vuilleumier Laurent[*]

[*] *Federal Office of Meteorology and Climatology MeteoSwiss, Payerne, Switzerland (daniel.walker@meteoswiss.ch)*
[**] *Institute for Atmospheric and Climate Science, ETH Zurich, Switzerland*

Ultraviolet (UV) radiation is known to have strong and potentially adverse effects on human health, ecosystems and materials. Erythemal UV irradiance has been defined as a measure to quantify such effects on human skin. The medical community and public health policy makers are interested in detailed information about the spatial distribution and temporal evolution of UV radiation.

UV time-series in Switzerland are spatially sparse and temporally too short to answer current needs including trend analyses. Therefore, radiative transfer models are used to substitute for missing data. However, simulating the effect of clouds on UV is very difficult, but being able to handle both clear-sky situations and various cloud conditions is crucial in assessing changes in UV radiation. An alternative way of describing the influences of clouds is the use of global shortwave radiation (SW_{glo}) as a proxy. This parameter holds information about the transmittance of the atmosphere and describes the cloud effect over the whole solar spectra. Furthermore, the advantages of SW_{glo} are the vast availability of measurements and the long time-series available in Switzerland.

We present a model that calculates global erythemal UV radiation for all-sky conditions. This model combines the accuracy of radiative transfer models for clear-sky conditions with semi-empiric information describing the influence of clouds. For this purpose cloud modification factors in the UV and SW range are inferred from data. The dependencies of this model on environmental conditions such as solar position, total ozone, and surface reflectance are analyzed. Resulting estimated UV doses are validated against UV observations at four locations in Switzerland. A fine time resolution of 10 minutes allows a validation of various aggregated UV doses (10', 1h, and daily doses).

The model is able to describe the short-term variability in the UV radiation due to changing cloud coverage. Depending on the location, RMS errors between 10.6 and 14.4% for the 10'-data have been found. The correlation exceeds 0.99. Better correspondence is obtained for daily UV doses with RMS errors between 6.3 and 9.5%. The performance of the method is generally better for higher solar elevations. The skills are lower at the high alpine station Jungfraujoch due to measurement problems, such as icing.